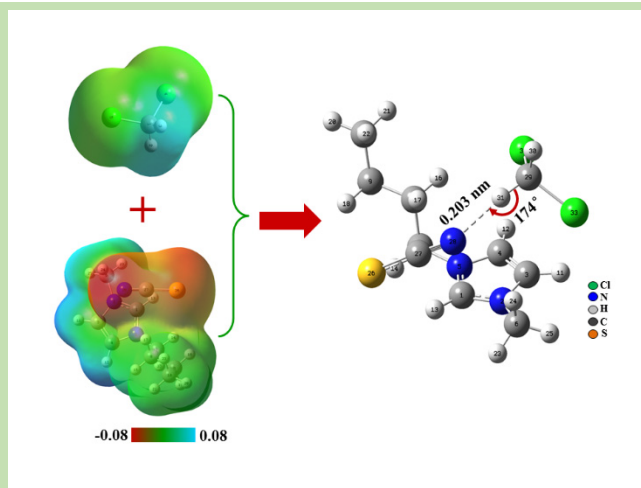# Efficient absorption of dichloromethane using imidazolium based ionic liquids

Wenliang WU[1,2], Tao LI[1], Hongshuai GAO[2*], Dawei SHANG[2], Wenhui TU[2], Binqi WANG[2], Xiangping ZHANG[1,2*]

1. School of Chemical Engineering and Energy, Zhengzhou University, Zhengzhou, Henan 450001, China
2. Beijing Key Laboratory of Ionic Liquids Clean Process, State Key Laboratory of Multiphase Complex System, Institute of Process Engineering, Chinese Academy of Sciences, Beijing 100190, China

Abstract: In recent years, environment problems have been a hot issue of concern to the public. Chlorinated volatile organic compounds such as dichloromethane (DCM) have been a serious threat to the public health and environment as hazardous chemical substances. Solving these problems has become an urgent issue in nowadays society. Ionic liquids (ILs) are supposed to be potential solvents to absorb gases due to their unique structures and properties, which have exhibited excellent absorption capacity in NH_3, SO_2, CO_2 and other gases. In this paper, a series of conventional ILs including [Bmim][BF$_4$], [Bmim][PF$_6$], [Bmim][DCA], [Bmim][SCN],

[Bmim][NTf$_2$], [Emim][SCN], [BPy][SCN] were synthesized and used as absorbents for dichloromethane (DCM) capture at different temperatures and partial pressures. The absorption capacities of DCM by ILs were measured by a highly sensible microbalance-intelligent gravimetric analyzer (IGA). It was found that [Bmim][SCN] has the highest absorption capacity to DCM (1.46 g/g, 303.15 K, 60 kPa) among these investigated ILs, and the absorption capacity of [Bmim][SCN] had no obvious decline after five absorption−desorption cycles. The densities and viscosities of [Bmim][SCN] with different mass fraction of DCM absorbed were measured in this work as well. And with the increase of the mass fraction of DCM absorbed, the density of DCM absorbed [Bmim][SCN] increased slightly, while the viscosity decreased dramatically. In addition, mechanism of DCM absorption by [Bmim][SCN] was investigated through FT-IR and [1]H−NMR, implying the interaction between DCM and [Bmim][SCN] was physical interaction. Furthermore, the interactions between cations or anions of ILs and DCM were investigated by quantum chemical calculation, which demonstrated that the anions of ILs had a more significant influence on the absorption capacity than cations, on account of the strong hydrogen bond interaction between anion and DCM, which has a great agreement with the results of experiment. This work will provide a new sight for designing more competitive ILs for DCM capture.
Key words: imidazolium ionic liquids; dichloromethane capture; absorption capacity; hydrogen bond

咪唑类离子液体高效吸收二氯甲烷

吴文亮 [1,2]，　李 涛 [1]，　高红帅 [2*]，　尚大伟 [2]，　涂文辉 [2]，　王斌琦 [2]，　张香平 [1,2*]

1. 郑州大学化工与能源学院，河南 郑州 450001
2. 中国科学院过程工程研究所离子液体清洁过程北京市重点实验室，多相复杂系统国家重点实验室，北京 100190

摘　要：合成了一系列常规离子液体 1-丁基-3-甲基咪唑四氟硼酸盐([Bmim][BF₄])、1-丁基-3-甲基咪唑六氟磷酸盐([Bmim][PF₆])、1-丁基-3-甲基咪唑双三氟甲磺酰亚胺盐([Bmim][NTf₂])、1-丁基-3-甲基咪唑双氰胺盐([Bmim][DCA])、1-丁基-3-甲基咪唑硫氰酸盐([Bmim][SCN])、1-乙基-3-甲基咪唑硫氰酸盐([Emim][SCN])和 N-丁基吡啶硫氰酸盐([BPy][SCN])，用智能重量分析仪(IGA)测定不同温度和分压下离子液体吸收二氯甲烷(DCM)的容量。结果表明，[Bmim][SCN]具有最高的二氯甲烷吸收容量(1.46 g/g, 303.15 K, 60 kPa)，5 次循环后吸收能力无明显下降，[Bmim][SCN]基本可完全再生，能循环使用。量化计算结果表明[SCN]⁻可与二氯甲烷形成氢键，增强其对二氯甲烷的吸收能力。

关键词：咪唑类离子液体；二氯甲烷捕集；吸收容量；氢键

中图分类号：X701.7　　　　**文献标识码：**A　　　　**文章编号：**1009–606X(2019)01–0173–08

1　INTRODUCTION

In recent years, volatile organic compounds (VOCs) such as dichloromethane (DCM) have attracted more and more concerns because they are considered as hazardous chemical substance and bring about serious threats to public health and environment[1–3]. DCM is widely used as a solvent for plastics, cellulose esters, fats, insecticides, paints, and so on[4]. It has been reported that DCM could increase the level of spontaneous abortions and the risk of cancer acquisition[5]. Therefore, how to deal with the emissions of DCM into the environment is a significant issue. Usually, the main method for the treatment of DCM is incineration, but it probably results in more hazardous byproducts than the original contaminants, such as phosgene. It is necessary to develop an effective technology for the removal of DCM from gas streams. Adsorption and absorption are the non-destructive techniques for the removal/recovery of VOCs from gas streams[2,6]. For example, Jesus et al.[7] reported that DCM could be removed from gas streams by means of fixed-bed adsorption with a commercial activated carbon. Zhou et al.[8] synthesized zirconium metal-organic framework UiO–66 and Al–fumarate metal-organic framework (MOF) nano-flakes and investigated their adsorption performance for DCM. UiO–66–5 showed a good DCM absorption capacity of 0.51 g/g at 298 K, which was higher than that of activated carbon (AC) with the absorption capacity of 0.20 mg/g[8,9]. However, the selectivity of these adsorbents is unsatisfactory and they are usually regenerated by heating at 573 K[6]. Accordingly, it is highly desired to develop a new adsorbent or absorbent for the efficient and easily reversible recovery of DCM from gas streams.

In the past decades, ionic liquids (ILs) have been revealed as promising media for the separation of various gases owing to their negligible volatility, excellent thermal stability, remarkable solubility and the variety of structures available[10,11]. According to significant work of predecessors, ILs have a great advantage to the absorption and desorption of inorganic gases, such as CO_2, SO_2, NH_3 and other industrial waste gases[12–18]. To our knowledge, there are very few studies on ILs for DCM removal or recovery. In this work, a series of imidazolium–based ILs with different anions and cations were synthesized, and their physicochemical properties as well as the absorption capacities of DCM were systematically investigated. In addition, the effect of temperature and partial pressure of DCM on the absorption performance, and the regeneration and recyclability of the [Bmim][SCN] were studied in detail. Moreover, the interaction mechanism between DCM and [Bmim][SCN] was explored by both experimental methods (FT-IR and ^{1}H-NMR spectroscopy) and molecular simulation.

2　EXPERIMENTS

2.1 Materials

[Emim][Cl], [Bmim][Cl], [BPy][Cl] were purchased from Linzhou Keneng Material Technology

Co., Ltd. Lithium bis(trifluoromethylsulfonyl)imide ($\geqslant$ 99%) were purchased from Aladdin Industrial Corporation. All other chemical reagents (AR), including dichloromethane, ethyl acetate, acetone, sodium nitrate, sodium fluoroborate, sodium dicyandiamide and sodium thiocyanate, were purchased from Beijing Chemical Company. All these chemical reagents above were used without further purification. Ultrapure water was obtained by the water purification system (Milli-Q Direct 8).

2.2 Synthesis of ILs

Imidazolium based ILs including 1-butyl-3-methylimidazolium bis(trifluoromethylsulfonyl) imide ([Bmim][NTf$_2$]), 1-butyl-3-methylimidazolium hexafluorophosphate ([Bmim][PF$_6$]), 1-butyl-3-methylimidazolium tetrafluoroborate ([Bmim][BF$_4$]), 1-butyl-3-methylimidazolium dicyandiamide ([Bmim][DCA]), 1-butyl-3-methylimidazolium thiocyanate ([Bmim][SCN]), 1-etyl-3-methylimidazolium thiocyanate ([Emim][SCN]), N-butylpyridinium thiocyanate ([BPy][SCN]), were synthesized through the anion exchange method and purified in our laboratory according to the reported methods[19–22]. All these ILs were dried under vacuum at 323.15 K for 48 h before usage.

2.3 Characterization and Physical Properties of ILs

The water contents of these ILs were measured by Karl Fisher coulometers C20 and had been reduced to less than 5×10^{-4}. The contents of residual chloride in the seven ILs were measured by PXSJ–226 Ion Analyzer (INESA Scientific Instrument Co., Ltd.) and they were all below 0.10 wt%. ^{1}H-NMR spectra were recorded on a Bruker spectrometer (600 MHz) in deuterated dimethyl sulfoxide (DMSO–d$_6$) with tetramethylsilane as the internal standard. The Fourier transform infrared (FT-IR) spectra were obtained in the range of 400~4000 cm^{-1} on a Thermo Nicolet 380 spectrometer. The ^{1}H NMR and FT-IR data were given in the Supplementary Material S1 and S2. The density and viscosity of [Bmim][SCN] with DCM were measured at temperatures from 283.15 K to 303.15 K with an interval of 5 K by a density meter (Anton Paar DMA 5000) and an automated microviscometer (Anton Paar Lovis 2000 M/ME), respectively.

2.4 Gas Solubility Apparatus and Measurement

The measurement of DCM solubility in ILs under different conditions were done using a computer-controlled Intelligent Gravimetric Analyzer (IGA, Hiden Isochema Ltd., Warrington, UK). The thermal coefficients of the weighting system was eliminated using a sensitive microbalance (accuracy of 0.1 μg), which could ensure the high accuracy of experimental data. ILs were degassed under a vacuum of less than 10^{-7} kPa at 353.15 K for 360 min prior to the adsorption measurement, which eliminated any existing water or organic solvent that may interfere with experiment. The experimental temperature was regulated within 0.1 K by a water bath. DCM was placed into a cylindrical iron bottle and heated to steam to be absorbed. The experimental pressure was increased gradually from 10^{-7} kPa to the setting pressure and continued to the absorption equilibrium using high accuracy Baratron pressure transducers. The changes of absorbent mass were continuously recorded and shown on the computer. Therefore, the absorption performance of ILs for DCM can be investigated by IGA with different partial pressure and different ambient temperature.

3　RESULTS AND DISCUSSION

3.1 Effect of Anions on Absorption Capacity

The absorption capacity of DCM in five kinds of imidazolium based ILs including [Bmim][SCN], [Bmim][BF$_4$], [Bmim][PF$_6$], [Bmim][DCA], [Bmim][NTf$_2$] were investigated under certain partial pressure from 4~60 kPa at 303.15 K were illustrated in Fig.1. It can be seen that the anions play a key role in determining the absorption capacities of DCM in ILs. It also indicated that the effect of anions on the absorption capacities of DCM on the basis of weight followed the order: [Bmim][SCN]>[Bmim][DCA]> [Bmim][BF$_4$]> [Bmim][PF$_6$]>[Bmim][NTf$_2$], which suggested that the absorption capacities of DCM decreased with increasement of the number of fluorine atoms in the anion. It was interesting to find that the solubility of CO$_2$ in [Bmim]$^+$ cation based ILs increased in the following order: [Bmim][DCA]< [Bmim][BF$_4$]<[Bmim][PF$_6$]< [Bmim][NTf$_2$] at 298 K[23], which indicated that CO$_2$ solubility increased with the number of fluorine atoms in

the anion increased. The reason can be explained as follow. Usually, the absorption capacity of gas in the ILs is determined by both the free volume of ILs and IL–gas interactions. For non-polar gases such as CO_2, the free volume of ILs plays a significant role in influencing the CO_2 solubility. While for polar gases such as DCM, the interaction between ILs and DCM played a primary role in gas solubility[24]. In these five imidazolium based ILs, [Bmim][SCN] had the highest absorption capacity for DCM, which may be due to the interaction between [SCN]⁻ and DCM are stronger than that of other anions. These results were further confirmed by the quantum chemistry calculations.
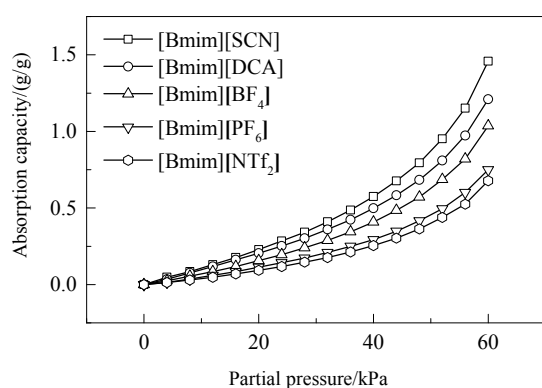

Fig.1   Absorption capacity of DCM by different imidazolium-based anions at 303.15 K and different DCM partial pressures

3.2 Effect of Cations on Absorption Capacity

In order to clarify cations or both anions and cations playing an important role in determining the absorption capacities of DCM in ILs, the effects of cations of ILs on the absorption capacity were investigated in this work. The absorption capacities of DCM in three ILs [Bmim][SCN], [Emim][SCN], [BPy][SCN] were measured under certain partial pressure from 4~60 kPa at 303.15 K and displayed in Fig.2. The results suggested that the absorption capacity of [Bmim][SCN] for DCM was slightly larger than that of [Emim][SCN] and [BPy][SCN], which could be mainly attributed to the larger cation size of the ILs. As the cation size increased, the Coulombic interaction between cation and anion decreased and the DCM could easily get access to the anion[25,26]. As a result, the interaction between anion and DCM will become stronger, and more DCM could be absorbed by ILs. In fact, though some slight differences

on the absorption capacities existed in these three ILs, the results indicated that the interaction between DCM and the cations was weak. In other words, the cations had a minor influence on the absorption capacity. Therefore, the major interaction involving DCM and the IL was more likely to occur between the anion and DCM. Because of the highest absorption capacity of [Bmim][SCN] for DCM, the [Bmim][SCN] was investigated as a typical example in the subsequent work.
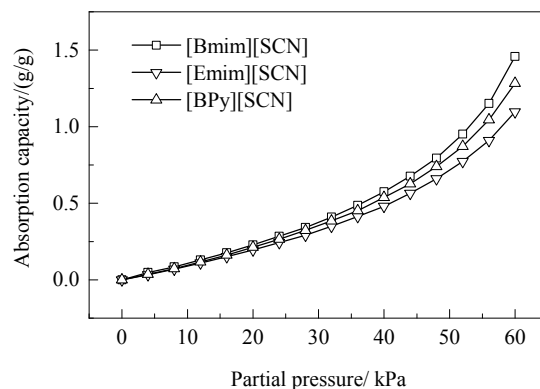

Fig.2   DCM absorption capacity of [Bmim][SCN], [BPy][SCN], [Emim][SCN] at 303.15 K and different DCM partial pressure

3.3 Effects of Absorption Temperature and Partial Pressure of DCM

The effects of temperature and partial pressure on the absorption capacity of [Bmim][SCN] for DCM were shown in Fig.3. It can be seen that the temperature and the partial pressure had key effects on the absorption amount of DCM. It also indicated that the absorption capacity of [Bmim][SCN] for DCM decreased continuously with the increasement of temperature. For example, the absorption capacity of [Bmim][SCN] for DCM decreases from 0.62 g/g to 0.23 g/g, when the temperature increased from 283.15 K to 303.15 K at 20 kPa. These results indicated that most of the absorbed DCM can be easily stripped out from [Bmim][SCN] by heating. Fig.3 presented that the absorption capacity of [Bmim][SCN] for DCM increases continuously with the increase of partial pressure. For example, the absorption capacity of [Bmim][SCN] for DCM increases from 0.05 g/g to 1.46 g/g, when the partial pressure increased from 4 to 60 kPa at 303.15 K. These results further suggested that it was preferable to absorb DCM at low temperature and high partial pressure of DCM.
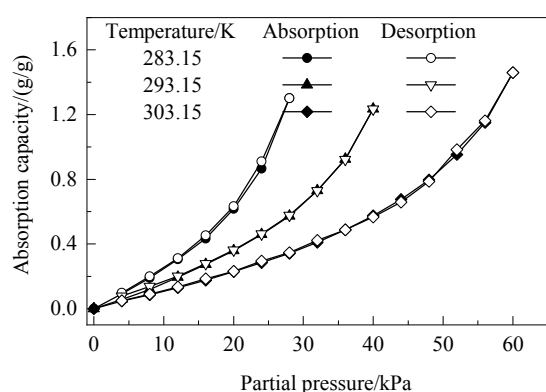
Fig.3　Absorption capacity of DCM by [Bmim][SCN]
at different temperature and DCM partial pressure

3.4 Physical Properties of [Bmim][SCN] with DCM

　　The densities and viscosities of [Bmim][SCN] with different mass fraction of DCM (0, 1%, 3%, 5%, 10%, 30%, 50%) were measured at the temperature ranging from 283.15 K to 303.15 K with an interval of 5 K in Fig.4.
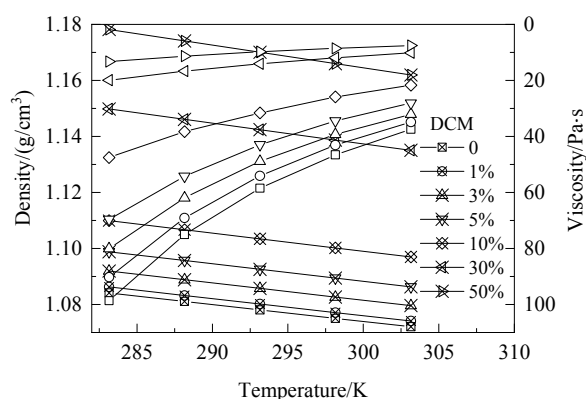

Fig.4　Density and viscosity of [Bmim][SCN] with different mass fraction of DCM at different temperature
(The hollow geometries represent viscosity and the hollow geometries with × represents density of [Bmim][SCN] with different mass fraction of DCM at different temperature)

　　As expected, the densities and viscosities of all the [Bmim][SCN] and DCM decreased with the increase of temperature. With the increase of the mass fraction of DCM, the density of DCM–absorbed [Bmim][SCN] increased slightly, while the viscosity decreased dramatically. DCM was captured by [Bmim][SCN] might decrease the Coulombic interactions between cation and anion of [Bmim][SCN], which caused the viscosity of the mixture of [Bmim][SCN] and DCM decreased greatly[25,26]. The viscosities of [Bmim][SCN] with different mass fraction of DCM can be fitted well by Arrhenius expression as the following equation[21,27]:

$$\eta = \eta_\infty \exp\left(\frac{-E_a}{RT}\right) \tag{1}$$

Where η is the viscosity at certain temperature, η_∞ is the viscosity at infinite temperature, E_a means viscosity activation energy, which indicates the difficulty that molecules can transfer through the liquid. The calculated viscosity activation energy of [Bmim][SCN] with certain mass fraction of DCM decreased with the mass fraction of DCM shown in the Table 1.

Table 1　The viscosity activation energy of [Bmim][SCN] with different mass fraction of DCM

The content of DCM/%	Viscosity activation energy E_a/(kJ/mol)
0	−34.458
1	−33.893
3	−32.638
5	−32.403
10	−27.964
30	−23.993
50	−20.108

3.5 [Bmim][SCN] Absorption–Desorption Cycles

　　The recyclability is an important factor to evaluatethe potential industrial application of ILs, thus five consecutive cycles of DCM absorption and desorption by [Bmim][SCN] were investigated. DCM absorption was carried out at 303.15 K and 4~60 kPa, whereas the desorption of DCM was vacuumized at 303.15 K and 60~4 kPa. As shown in Fig.5, the absorption capacity of [Bmim][SCN] for DCM had no obvious change after five cycles, which indicated that DCM could be desorbed easily and the DCM absorption–desorption process was highly reversible. However, it was reported that the activity of activated carbon (AC) decreased and secondary pollution was caused after regeneration of AC[6,28]. ILs may have an obviously advantageous than
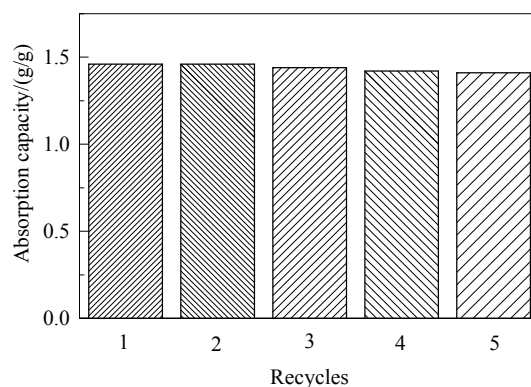

Fig.5　Five consecutive cycles of DCM absorption and desorption of [Bmim][SCN] at 303.15 K

AC considering environment and economy.

3.6 Mechanism of DCM Absorption

The interaction mechanism between ILs and DCM was further investigated by the analysis of FT-IR and ^{1}H-NMR spectra of [Bmim][SCN] before and after the absorption of DCM. The FT-IR spectra of DCM, fresh [Bmim][SCN] and DCM-absorbed [Bmim][SCN] as well as [Bmim][SCN] of desorption are displayed in Fig.6. Comparing with the FT-IR spectra of fresh [Bmim][SCN], there were two new absorption peaks observed in the FT-IR spectra of DCM-absorbed [Bmim][SCN] than the fresh [Bmim][SCN]. The two distinct absorption peaks were C–H with the external bending vibration at 1265 cm^{-1} and the stretching vibration peak of C–Cl at 733 cm^{-1}. It also showed that the peaks of 1267 cm^{-1}, 739 cm^{-1} shifted to 1265 cm^{-1}, 733 cm^{-1}, respectively after the uptake of DCM by [Bmim][SCN], which exhibited a red shift of the DCM, implying the presence of (DCM) C–H·and N hydrogen bonding interaction between anion ([SCN]$^-$) and DCM[29,30]. Meanwhile, there was a bump at 745 cm^{-1} on the C–Cl peak of DCM absorbed by [Bmim][SCN] that had a good agreement with the fresh [Bmim][SCN] at 745 cm^{-1} of CH$_2$(N) and CH$_3$(N)CN bend, which illustrated that there had an overlap between the peak of C–Cl and CH$_2$(N) and CH$_3$(N)CN bend[31]. New peaks appeared and disappeared while DCM was captured and desorbed, which suggest that [Bmim][SCN] absorbed DCM through physical interaction.

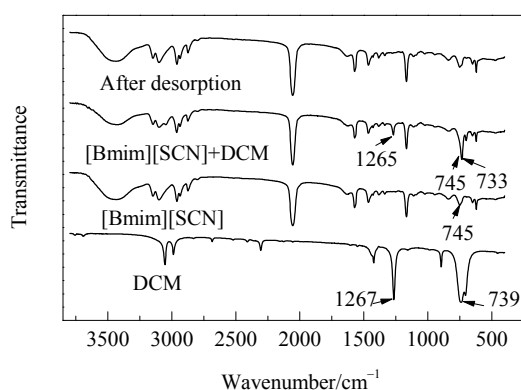Fig.6   FT-IR spectra of [Bmim][SCN] before and after absorption of DCM

Furthermore, the ^{1}H-NMR spectra of [Bmim][SCN] before and after absorption of DCM were studied further. Obviously, ^{1}H-NMR spectra of [Bmim][SCN] before and after absorption of DCM had no distinct changes in chemical shifts in Fig.7, implying that there was no new chemical bond formed between [Bmim][SCN] and DCM. According to the spectra, the peaks of before and after uptake of DCM had a very slight chemical shifts, which indicated the interaction between [Bmim][SCN] and DCM were very weak and mainly governed by physical interaction. In this context that hydrogen bond may be formed between ILs and DCM after absorption.
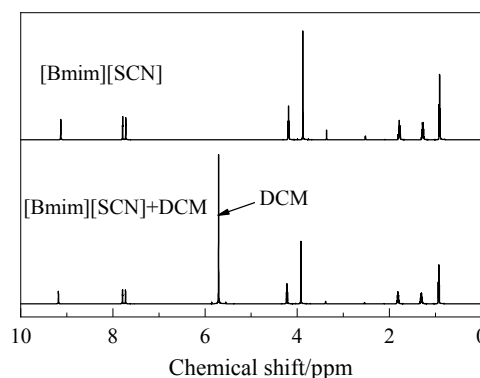

Fig.7   ^{1}H NMR spectra of [Bmim][SCN] before and after absorption of DCM

To further uncover the absorption mechanism of DCM by ILs, the interactions between cations or anions and DCM were investigated by quantum chemistry calculations at the level of B3LYP/6–311++G** with Gaussian 09 software. The interaction structures of cation, anion and IL–DCM were adjusted to the optimum structure and interaction energies of cations, anions and IL–DCM were displayed in Tables 2 and 3. The total interaction energies of [Bmim][SCN], [Bmim][DCA], [Bmim][BF$_4$], [Bmim][PF$_6$], [Bmim][NTf$_2$] with DCM were –48.82, –45.31, –42.18, –41.26, –32.14 kJ/mol, respectively, following the order of [Bmim][SCN]>[Bmim][DCA]>[Bmim][BF$_4$]> [Bmim][PF$_6$]>[Bmim][NTf$_2$], which was in good agreement with the order of the absorption performance of imidazolium–based ILs. According to the results of optimum structure between [Bmim][SCN] and DCM, the distances of H and N (0.203 nm) is shorter than Van der Waals distance of 0.267 nm between [SCN]$^-$ and DCM[32]. Furthermore, it showed that anion had a stronger interaction with DCM considering monomer interaction energies, because of hydrogen bonds between anion and DCM. And it further confirms that the anions

had a primary effect on the absorption performance and the optimum interaction structure showed in Fig.8.

Table 2　Interaction energies of ILs−DCM

IL−DCM	Interaction energy/(kJ/mol)
[Bmim][SCN]−DCM	−48.82
[Bmim][DCA]−DCM	−45.31
[Bmim][BF$_4$]−DCM	−42.18
[Bmim][PF$_6$]−DCM	−41.26
[Bmim][NTf$_2$]−DCM	−32.14

Table 3　Interaction energies between ions of ILs and DCM

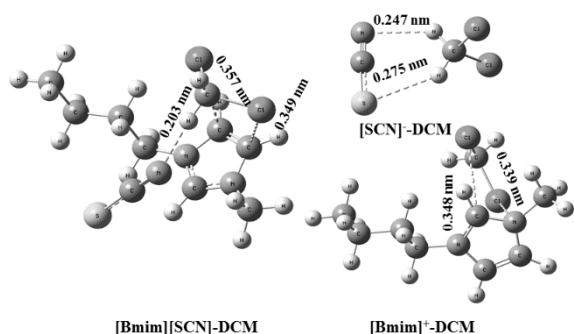| Ion−DCM	Interaction energy/(kJ/mol)
[Bmim]−DCM	−35.91
[SCN]−DCM	−53.13
[DCA]−DCM	−44.73
[BF$_4$]−DCM	−51.87
[PF$_6$]−DCM	−46.61
[NTf$_2$]−DCM	−47.57

Fig.8　The optimum structures between [Bmim]$^+$, [SCN]$^-$, [Bmim][SCN] and DCM

4　CONCLUSION

In summary, a series of conventional imidazolium based ILs were synthesized and used as effective absorbents to capture and recover DCM. The absorption capacity of ILs for DCM and the physical properties of ILs with DCM were investigated in detail:

(1) [Bmim][SCN] had the highest absorption capacity (1.46 g/g at 303.15 K, 60 kPa) among these seven ILs.

(2) The hydrogen bond interaction between anion and DCM presented an important effect on the absorption capacity of ILs.

(3) [Bmim][SCN] revealed a great recycle performance without a significant absorption capacity decrease after five recycles for DCM, which indicated the stable and reusable capacity of [Bmim][SCN].

(4) With advantages of high absorption capacity, excellent cyclic utilization and less pollution, [Bmim][SCN] might be a promising solvents for capture organic chlorides.

REFERENCE

[1] Ozturk B, Yilmaz D. Absorptive removal of volatile organic [J]. Process Safety and Environment Protection, 2006, 84(B5): 391–398.

[2] Yun J H, Choi D K. Adsorption equilibria of chlorinated organic solvents onto activated carbon [J]. Industrial and Engineering Chemistry Research, 1998, 37(4): 1422–1427.

[3] Schlosser P M, Bale A S, Gibbons C F, et al. Human health effects of dichloromethane: key findings and scientific issues [J]. Environmental Health Perspectives, 2015, 123(2): 114–119.

[4] Yu J M, Cai W J, Chen J M, et al. Conversion characteristics and mechanism analysis of gaseous dichloromethane degraded by a VUV light in different reaction media [J]. Journal of Environmental Sciences, 2012, 24(10): 1777–1784.

[5] Shestakova M, Sillanpaa M. Removal of dichloromethane from ground and wastewater: a review [J]. Chemosphere, 2013, 93(7): 1258–1267.

[6] Borkar C, Tomar D, Gumma S. Adsorption of dichloromethane on activated carbon [J]. Journal of Chemical and Engineering Data, 2010, 55: 1640–1644.

[7] Lemus J, Martin-Martinez M, Palomar J. Removal of chlorinated organic volatile compounds by gas phase adsorption with activated carbon [J]. Chemical Engineering Journal, 2012, 211/212: 246–254.

[8] Zhou L, Zhang X H, Chen Y L. Facile synthesis of Al-fumarate metal–organic framework nano-flakes and their highly selective adsorption of volatile organic compounds [J]. Materials Letters, 2017, 197: 224–227.

[9] Zhou L, Zhang X H, Chen Y L. Modulated synthesis of zirconium metal–organic framework UiO-66 with enhanced dichloromethane adsorption capacity [J]. Materials Letters, 2017, 197: 167–170.

[10] Leng Y, Wang J, Zhu D R, et al. Heteropolyanion-based ionic liquids: reaction-induced self-separation catalysts for esterification [J]. Angewandte Chemie International Edition, 2009, 48(1): 168–171.

[11] Dong K, Liu X M, Dong H F, et al. Multiscale studies on ionic liquids [J]. Chemistry Reviews, 2017, 117(10): 6636–6695.

[12] Shang D W, Zhang X P, Zeng S J, et al. Protic ionic liquid [Bim][NTf$_2$] with strong hydrogen bond donating ability for highly efficient ammonia absorption [J]. Green Chemistry, 2017, 19(4): 937–945.

[13] Zeng S J, Wang J, Bai L, et al. Highly selective capture of CO$_2$ by ether-functionalized pyridinium ionic liquids with low viscosity [J]. Energy Fuels, 2015, 29(9): 6039–6048

[14] Che S Y, Dao R N, Zhang W D, et al. Designing an anion-functionalized fluorescent ionic liquid as an efficient and reversible turn-off sensor for detecting SO$_2$ [J]. Chemical Communications, 2017, 53(27): 3862–3865.

[15] Yang D Z, Han Y L, Qi H B, et al. Efficient absorption of SO$_2$ by EmimCl-EG deep eutectic solvents [J]. ACS Sustainable Chemistry & Engineering, 2017, 5(8): 6382–6386.

[16] Zeng S J, Zhang X C, Gao H S, et al. SO$_2$-induced variations in the viscosity of ionic liquids investigated by *in situ* fourier transform infrared spectroscopy and simulation calculations [J]. Industrial and Engineering Chemistry Research, 2015, 54(43): 10854–10862.

[17] Wang J F, Petit C, Zhang X P, et al. Simultaneous measurement of CO$_2$ sorption and swelling of phosphate-based ionic liquid [J]. Green Energy & Environment, 2016, 1(3): 258–265.

[18] Meng X C, Wang J Y, Jiang H C, et al. Guanidinium-based dicarboxylic acid ionic liquids for SO$_2$ capture [J]. Journal of

Chemical Technology and Biotechnology, 2017, 92(4): 767–774.

[19]   Liu X Y, Huang Y, Zhao Y S, et al. Ionic liquid design and process simulation for decarbonization of shale gas [J]. Industrial and Engineering Chemistry Research, 2016, 55(20): 5931–5944.

[20]   Zeng S J, Gao H S, Zhang X P, et al. Efficient and reversible capture of SO_2 by pyridinium-based ionic liquids [J]. Chemical Engineering Journal, 2014, 251: 248–256.

[21]   Li Z J, Zhang X P, Dong H F, et al. Efficient absorption of ammonia with hydroxyl-functionalized ionic liquids [J]. RSC Advances, 2015, 5(99): 81362–81370.

[22]   Shang D W, Bai L, Zeng S J, et al. Enhanced NH_3 capture by imidazolium-based protic ionic liquids with different anions and cation substituents [J]. Journal of Chemical Technology and Biotechnology, 2018, 93(5): 1228–1236.

[23]   Lei Z G, Han J L, Zhang B F, et al. Solubility of CO_2 in binary mixtures of room-temperature ionic liquids at high pressures [J]. Journal of Chemical and Engineering Data, 2012, 57(8): 2153–2159.

[24]   Lei Z G, Dai C N, Chen B H. Gas solubility in ionic liquids [J]. Chemistry Reviews, 2014, 114(2): 1289–1326.

[25]   Ando R A, Siqueira L J A, Bazito F C, et al. The sulfur dioxide-1-butyl-3-methylimidazolium bromide interaction: drastic changes in structural and physical properties [J]. Journal of Physical Chemistry B, 2007, 111(30): 8717–8719.

[26]   Ren S H, Hou Y C, Wu W Z, et al. Properties of ionic liquids absorbing SO_2 and the mechanism of the absorption [J]. Journal of Physical Chemistry B, 2010, 114(6): 2175–2179.

[27]   Brown P, Gurkan B E, Hatton T A. Enhanced gravimetric CO_2 capacity and viscosity for ionic liquids with cyanopyrrolide anion [J]. AIChE Journal, 2015, 61(7): 2280–2285.

[28]   Feldheim D L, Hendrickson S M, Krejcik M, et al. Kinetics of dichloromethane absorption into the conductive polymers [J]. Journal of Physical Chemistry, 1995, 99(10): 3288–3293.

[29]   Borisch J, Pilkenton S, Miller L M, et al. TiO_2 photocatalytic degradation of dichloromethane: an FTIR and solid-state NMR study [J]. Journal of Physical Chemistry B, 2004, 108(18): 5640–5646.

[30]   Ding F, He X, Luo X Y, et al. Highly efficient CO_2 capture by carbonyl-containing ionic liquids through lewis acid-base and cooperative C−HO hydrogen bonding interaction strengthened by the anion [J]. Chemical Communications, 2014, 50(95): 15041–15044.

[31]   Noack K, Schulz P S, Paape N, et al. The role of the C2 position in interionic interactions of imidazolium based ionic liquids: a vibrational and NMR spectroscopic study [J]. Physical Chemistry Chemical Physics, 2010, 12(42): 14153–14161.

[32]   Meng Z, Dolle A, Carper W R. Gas phase model of an ionic liquids: semi-empirical and Ab initio bonding and molecular structure [J]. Journal of Molecular Structure: Theochem, 2002, 585: 119–128.